Polymerization-Induced Self-Assembly via RAFT in Emulsion: Effect of Z-Group on the Nucleation Step

Thiago R. Guimarães,[1] Yuen L. Bong,[1] Steven W. Thompson,[1] Graeme Moad,[2] Sébastien Perrier[3,4,5] and Per B. Zetterlund[1,*]

[1] Centre for Advanced Macromolecular Design (CAMD), School of Chemical Engineering, The University of New South Wales, Sydney, NSW, 2052, Australia.

[2] CSIRO Manufacturing Flagship, Bag 10, Clayton South, VIC 3169, Australia.

[3] Department of Chemistry, University of Warwick, Coventry, CV4 7AL, UK.

[4] Warwick Medical School, University of Warwick, Coventry, CV4 7AL, UK

[5] Faculty of Pharmacy and Pharmaceutical Sciences, Monash University, 381 Royal Parade, Parkville, Victoria 3052, Australia

ABSTRACT

Polymerization-Induced Self-Assembly (PISA) has emerged as one of the most powerful and widely employed techniques for preparation of block copolymer and polymeric nanoparticles in dispersed systems. Its success relies on a rapid, easily scalable and straightforward process, associated with the ability to readily control nanoparticle morphology. In the present work, we have investigated effect of the Z-group on the nucleation step of aqueous RAFT PISA performed in environmentally friendly emulsion polymerization. Seven different poly(acrylic acid) (PAA) and poly(methacrylic acid) (PMAA) macroRAFTs were synthesized using RAFT agents containing Z-groups of different hydrophilicity. Slow polymerizations and incomplete chain extension reactions were observed for systems with a hydrophilic Z-group, while the more hydrophobic Z groups led to higher polymerization rates and very successful chain extensions. A mechanism based on Z-group induced RAFT exit is proposed to rationalize this surprisingly behaviour, providing important information on the mechanistic understanding and optimization of PISA in emulsion.

INTRODUCTION

Polymerization-Induced Self-Assembly (PISA) has been attracting increasing interest in polymer synthesis in the last decade as an efficient method for the production of block copolymer nano-objects of various morphologies.[1-7] The approach typically entails synthesis of a macromolecule that is soluble in a suitable solvent via reversible deactivation radical polymerization (RDRP), followed by chain extension with a second monomer forming amphiphilic chains which self-assemble into nano-objects. Note however that PISA can also be conducted based on non-living radical polymerization as exemplified by addition-fragmentation chain transfer (AFCT) polymerization.[8] The PISA process is attractive as it enables control of the particle morphology not only as conventional spherical particles but also sophisticated morphologies such as fibers, vesicles, jellyfish, 'yolk/shell', multi-shelled vesicles, *etc*. Furthermore, PISA processes also present the advantages of high polymerization rate with no intermediate purification steps, and the resulting dispersions can be obtained with high solids contents (30-50%).

Reversible Addition-Fragmentation chain Transfer (RAFT) polymerization is the RDRP technique by far most commonly used for implementation of PISA due to the great versatility of RAFT polymerization towards a wide range of monomers, and also its

compatibility with various solvents, including water.[9-11] The preparation of various amphiphilic block copolymers self-assembling into sophisticated morphologies has been the focus of numerous studies combining both processes (RAFT and PISA)[12-18] with potential applications in the field of drug delivery,[12, 13] cell culture,[12] coatings technologies[14, 15] and responsive films.[1, 16, 17] Recently, nano-objects with controlled morphology have also been synthesized via PISA in dispersion polymerization with the hydrophilic block composed of stimuli-responsive polymer.[19, 20] The morphology can be readily tuned (spheres, worms or vesicles) by external stimuli such as pH,[19] ionic strength[19] or CO_2 pressure,[20] without altering the formulation. Besides being a direct and straightforward method to easily control the morphology, this strategy also allows the preparation of nano-objects with different morphologies from block copolymers exhibiting exactly the same composition – generally the morphology of the nano-objects is tuned by changing the length and/or the composition of each block.

PISA, most commonly conducted as a dispersion polymerization in water/alcohol, can also be conducted in environmentally friendly emulsion polymerization which uses water as the continuous phase. Emulsion PISA is also a readily industrially scalable technique - conventional emulsion polymerization is a well-established industrial process.[3, 5] The pioneering work on PISA in emulsion was first reported by Ferguson *et al.*[21, 22] A hydrophilic macroRAFT agent was synthesized via RAFT solution polymerization in dioxane. The purified macroRAFT was subsequently chain extended in aqueous phase with a hydrophobic monomer leading to self-assembly into polymer particles. Chaduc *et al.*[23] simplified this process by preparing both the hydrophilic and the hydrophobic blocks in the same batch in water, thereby eliminating the time-consuming steps of preparation and purification of the hydrophilic macroRAFT agent. This strategy was explored using various hydrophilic macroRAFTs such as poly(acrylic acid) (PAA),[24] poly(methacrylic acid) (PMAA),[25] and others.[26, 27] The effects of pH, hydrophobic monomer, molecular weight of hydrophilic and hydrophobic blocks and concentration of macroRAFT have been investigated in detail. Interestingly, fluorescence studies of PMAA and PAA macroRAFTs using the solvatochromic dye Nile red revealed very different behaviour in aqueous solution. PMAA exhibited a hyper-coiled structure at low pH whilst PAA did not, which would affect the mechanism of PISA. The presence of a hyper-coiled structure at low pH for PMAA systems generates hydrophobic domains in the early stages of polymerization, which results in an increase in the local concentration of hydrophobic monomer (second block). Therefore, the formation of amphiphilic block copolymer is more rapid and, consequently, so is the nucleation process (ca. 30 min) compared to the corresponding PAA system, in which more than 3 h of inhibition period was observed.[24, 25] Early works on PISA performed in emulsion polymerization generally resulted in spherical particles. In contrast, sophisticated morphologies have been readily obtained via dispersion polymerization. Recently, Armes and co-workers[28, 29] have proposed that this is associated with the increased ability of the monomer to swell the polymer in dispersion polymerization, thereby facilitating chain mobility and, consequently, the phase transition from particles to worms, vesicles and so on.

Herein, we have explored the effect of the Z-group hydrophobicity on the kinetics of the RAFT PISA in emulsion polymerization. Seven different PAA- and PMAA-based macroRAFTs were synthesized via RAFT polymerization using RAFT agents containing Z-groups of different hydrophilicity. Previously, in a very recent paper, we investigated[30] the aqueous phase conformation of these PMAA- and PAA-based macroRAFTs. These hydrophilic macroRAFTs were subsequently employed in aqueous PISA of styrene. Kinetics studies demonstrated that the nucleation step can be strongly affected by even very minor changes in the structure of the Z-group.

EXPERIMENTAL

Materials

The RAFT agents (Scheme 1) 4-((((2-carboxyethyl)thio)carbonothioyl)thio)-4-cyanopentanoic acid (RAFT1, >95%), 4-cyano-4-((dodecylsulfanylthiocarbonyl)sulfanyl)pentanoic acid (RAFT3, >97%) and 2-(((dodecylthio)carbonothioyl)thio)propanoic acid (RAFT5, >97%) were all purchased from Boron Molecular and used as received. The RAFT agents 4-cyano-4-thiothiobutylsulfanylpentanoic acid (RAFT2)[30] and 2-(((butylthio)carbonothioyl)thio)-2-methylpropanoic acid[31] were synthesized according to reported protocols.[30, 31] The initiators potassium persulfate (KPS, Sigma-Aldrich) and 4,4'-azobis(4-cyanopentanoic acid) (ACPA, Wako) were used as received. Methacrylic acid (MAA, Sigma-Aldrich) and acrylic acid (AA, Sigma-Aldrich) were used with no further purification. Styrene (Sty, >99%, Sigma-Aldrich) was passed through basic alumina to remove the inhibitor before use. Tri(methylsilyl)diazomethane was used as methylation agent (Sigma-Aldrich). Deuterated solvents chloroform ($CDCl_3$) and deuterium oxide (D2O) were used for NMR analysis, both obtained from Novachem. Deionized (DI) water was obtained by a Milli-Q reverse osmosis system with a resistivity of 18.2 mΩ cm^{-1}.

Synthesis of hydrophilic macroRAFT

In a typical experiment, 1.18 mmol of RAFT agent (RAFT3), 4.73 mmol of 1,3,5-trioxane, 56.9 mmol of AA and 0.0594 mmol of ACPA were introduced in a 25ml glass vial (Table SI1). The mixture was diluted with 15 mL of 1,4-dioxane. The [RAFT]/[I] and [M]/[RAFT] ratios were 20 and 44, respectively (unless otherwise stated), and solids content 24%. The flask was septum-sealed and purged with nitrogen for 30 min, and then immersed in an oil bath at 80°C with magnetic stirring at 300rpm. The reaction was conducted overnight. Conversion was calculated using NMR analysis and number average molecular weight (M_n) and dispersity ($Đ$) determined by SEC-THF. The theoretical molecular weight ($M_{n,th}$) was calculated according to the equation:

$$M_{n,theo} = \frac{[Mon]_0 \cdot M_{Mon} \cdot X}{[RAFT]_0} + M_{RAFT} \qquad (1)$$

where $[M]_0$ and $[RAFT]_0$ are the initial monomer and RAFT concentrations, respectively, M_M is the molar mass of the monomer, X is the fractional conversion of monomer and M_{RAFT} is the molar mass of the macroRAFT agent. The livingness was calculated based on the equation:

$$L = \frac{[CTA]_0}{[CTA]_0 + 2 \times f \times [I]_0 \times (1 - e^{-k_d t}) \times (1 - \frac{f_c}{2})} \qquad (2)$$

where $[CTA]_0$ and $[I]_0$ are the initial concentrations of the RAFT agent and initiator, respectively, and f_c is the coupling factor (termination by disproportionation was assumed for PMAA, $f_c = 0$, while for PAA coupling was assumed, $f_c = 1$). The term $2 \times f \times [I]_0 \times (1 - e^{-k_d t})$ corresponds to the total number of radicals generated from the initiator over the polymerization time, where f is the initiator efficiency (assumed to be 0.6) and k_d is the rate constant of decomposition for ACPA ($k_d = 1.26 \times 10^{16} \times e^{-134/RT}\ s^{-1}$).[32]

The macroRAFTs prepared in aqueous solution were used without purification. The macroRAFTs prepared in dioxane were purified by precipitating three times. The first precipitation was conducted directly from the reaction medium in cyclohexane. Two extra precipitations were performed using 5 ml of methanol as solvent and 50 ml diethyl ether as

non-solvent. The polymer was recovered via centrifugation at 9000 rpm for 3 min. The purified macroRAFT (light-yellow fine powder) was obtained after drying in a high vacuum oven at 30ºC.

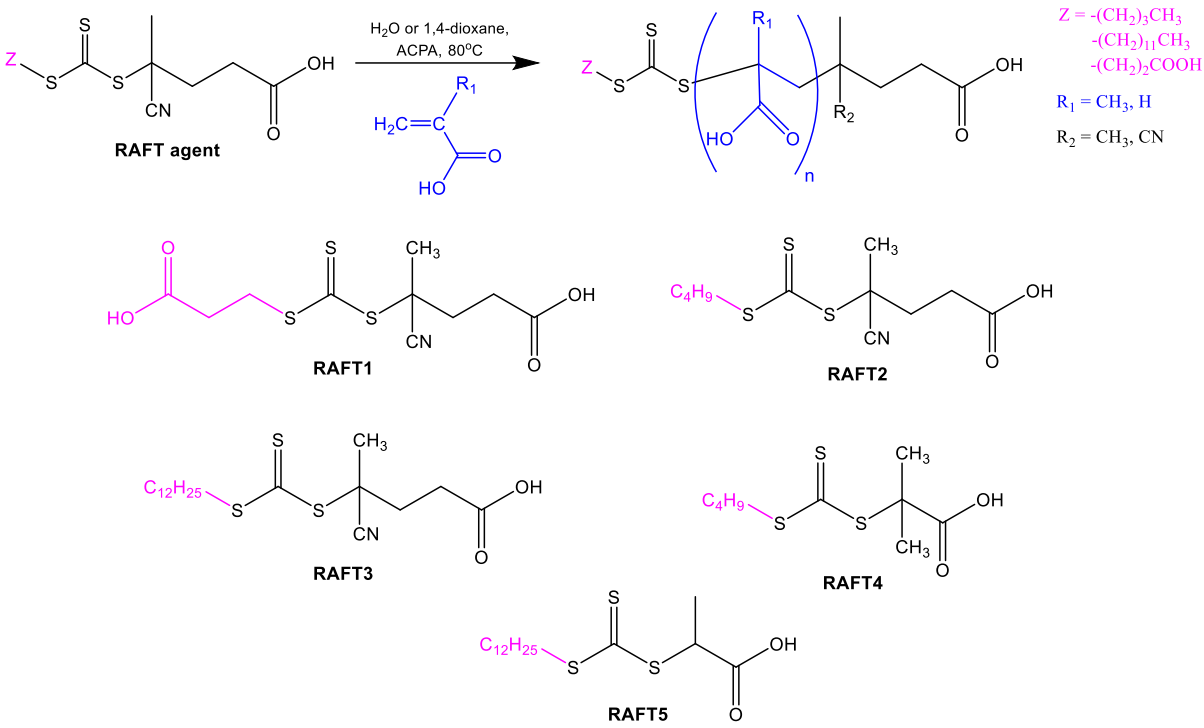

Scheme 1 – Synthesis of hydrophilic macroRAFT agents via RAFT solution polymerization (Table S1).

PISA via RAFT emulsion polymerization

In a typical experiment (Latex 2, Table 1), 5 g of pre-synthesized macroRAFT solution ($PMAA_{43}$-Ac, 1.2 10^{-2} mol L^{-1}), 4 mL of deionized water, 2.4 g of styrene and 1 mL of KPS stock solution (2.3 10^{-3} mol L^{-1}) were added into a 25 mL glass flask. The [M]/[RAFT] and [RAFT]/[I] ratios were kept at 200 and 5, respectively, and solids content = 22% (Table 1). The flask was septum-sealed with parafilm and wire, and purged with nitrogen for 30 min in an ice-water bath. After degassing, the flask was transferred to a thermostatically controlled oil bath pre-heated at 80°C under magnetic stirring of 500 rpm. The polymerization was conducted for 6h (unless otherwise stated). Samples were periodically withdrawn with a degassed needle to monitor conversion by gravimetry, particle size by DLS, M_n and $Đ$ by SEC.

Size exclusion chromatography (SEC)

M_n and $Đ$ were determined using a Shimadzu modular system using tetrahydrofuran (THF, HPLC grade, Chem Supply) at 40 °C and 1 mL min^{-1} as the mobile phase equipped with an auto-injector Shimadzu SIL-10AD, 5.0 µm bead size guard column from Polymer Laboratories (50x7.5 mm^2), 4 linear PL (Styragel) columns (105, 104, 103 and 500 Å), differential refractive index detector (RI, RID-10A RI) and UV detector (SPD-20AV). Prior to SEC analyses, the carboxylic acid groups of the polymer were methylated in a THF/H_2O (90/10) mixture using (trimethylsilyl)diazomethane solution (Sigma-Aldrich) as the methylation agent. The system was calibrated with PS standards (ranging from 580 to 1,037,000 g mol^{-1}) or PMMA standards (ranging from 885 to 1,020,000 g mol^{-1}).

Dynamic light scattering (DLS)

Intensity mean average diameter (Z_{av}) and polydispersity index (PdI) were measured using a Malvern Zetasizer Nanoseries (NanoZS). Measurements were conducted at 25°C using a 4 mW He-Ne laser with wavelength 633 nm, and a scattering angle of 173°. Samples for analysis were prepared by diluting 1 drop of the latex with deionized Milli-Q water. Z_{av} and PdI were obtained using the fully automatic mode of the Zetasizer system and fitted with monomodal cumulant analysis.

RESULTS

The main focus of the present work has been to investigate to what extent the hydrophilicity of the Z-group of the RAFT agent affects the mechanism of PISA in emulsion polymerization. The one-pot PISA process adopted is based on the strategy reported by Chaduc *et al.*[23] Hydrophilic PMAA- and PAA-based macroRAFT agents with different Z-groups (Table S1 and Figure 1) were prepared via solution polymerization in water (except $PMAA_{38}$-C12 and PAA_{46}-C12 macroRAFTs, which were synthesized in dioxane due to poor water solubility of the RAFT agent). All polymerizations proceeded under RAFT control resulting in low dispersities ($Đ$ = 1.1~1.2, Table S1) with monomodal and well-defined molecular weight distributions (MWDs; Figure 1). The degree of livingness was calculated according to equation 2, resulting in very high chain end-fidelity (L > 94%, Table S1). These macroRAFTs were subsequently chain extended with styrene, leading to self-assembly into polymer particles.

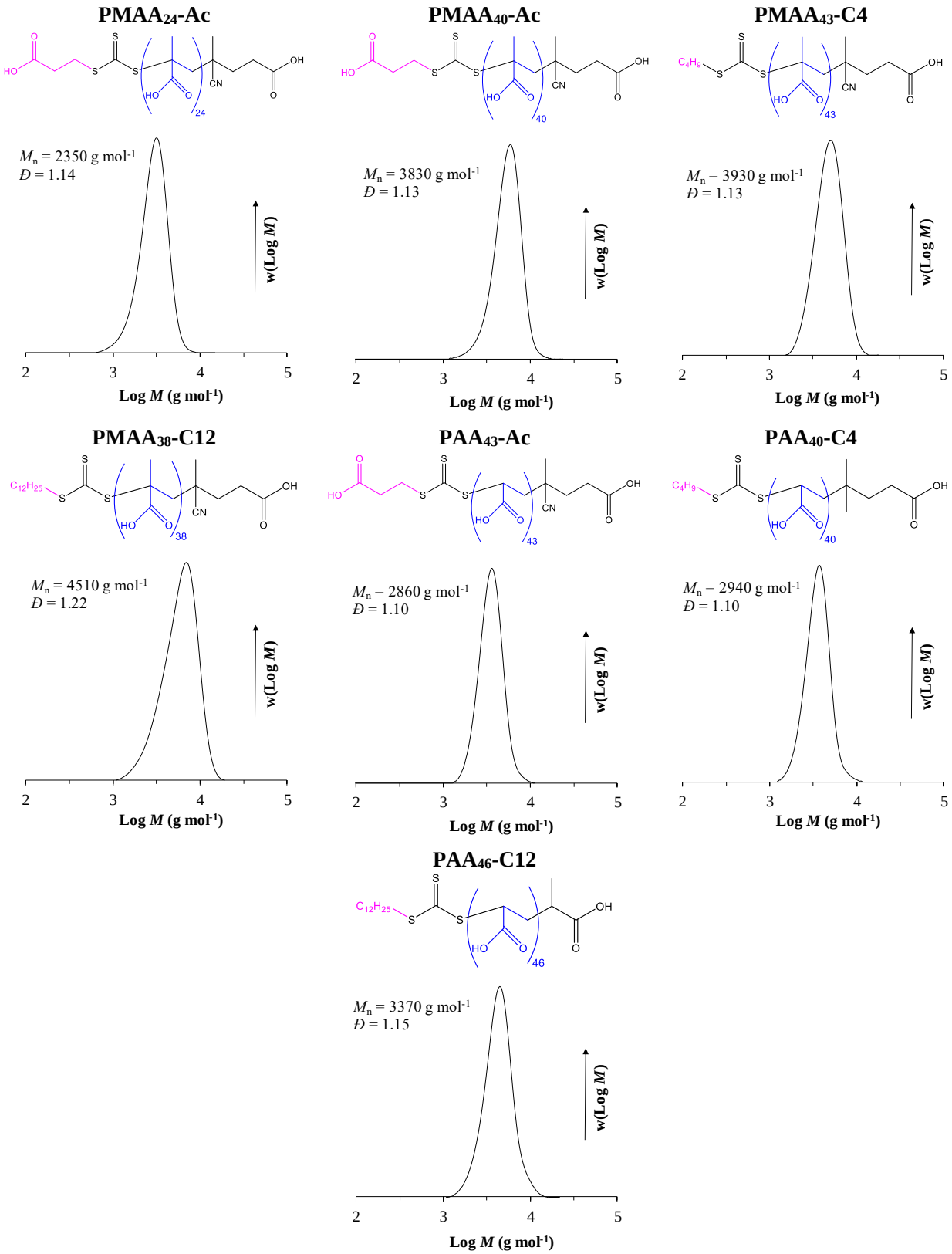

Figure 1 – Structures of PMAA- and PAA-based macroRAFTs synthesized using RAFT agents with different Z-groups.

PMAA-based system: Effect of Z-group hydrophobicity

Initially we focus our attention on PISA of styrene mediated by PMAA-based macroRAFT agents with different Z-groups. The experimental conditions and the results are summarized in Table 1. The experiments performed in the presence of the $PMAA_{40}$-Ac macroRAFT (Latex 2) exhibited unexpected behaviour in terms of kinetics compared to $PMAA_{43}$-C4 (Latex 3; Figure 2A). The emulsion polymerization in the presence of $PMAA_{43}$-C4 proceeded very fast, reaching full conversion in 1h, resulting in small particle size (Z_{av} = 71 nm), in agreement with previous work[25] performed with a similar macroRAFT agent ($PMAA_{43}$-C3, Z-group: -S-CH_2-CH_2-CH_3). On the contrary, $PMAA_{40}$-Ac resulted in much lower polymerization rate with only 53% conversion in 6h and significantly larger particles (Z_{av} = 190 nm). These two macroRAFTs have very similar structures ($PMAA_{40}$-Ac and $PMAA_{43}$-C4; Figure 1), composed of ca. 40 units of methacrylic acid and the same R-group. The main difference is the additional carboxylic acid group of the Z-group for $PMAA_{40}$-Ac (Figure 2). This seemingly very minor difference in structure drastically affects the kinetics of emulsion polymerization. Furthermore, the control of the MWD was also negatively impacted with incomplete consumption of $PMAA_{40}$-Ac, while $PMAA_{43}$-C4 resulted in successful chain extension (Figure 3B and 3C). How does this minor change in RAFT agent structure so dramatically influence the polymerization?

Table 1 – Emulsion polymerization of styrene mediated by PMAA- and PAA- based macroRAFT agents with different Z-groups.[a]

Exp	*MacroRAFT*	*X (%)/ t(h)*[b]	$M_{n,theo}$ *(g mol*$^{-1}$*)*[c]	M_n */Đ (g mol*$^{-1}$*)*[d]	Z_{av}*/Poly (nm)*[e]	N_p *(L*$^{-1}$*)*[f]
Latex 1	$PMAA_{20}$-Ac	50/6.0	11,800	16,150/3.51	184/0.02	3.5 10^{16}
Latex 2	$PMAA_{40}$-Ac	53/5.9	15,250	29,700/2.11	190/0.02	4.8 10^{16}
Latex 3	$PMAA_{43}$-C4	100/1.3	25,700	21,900/1.29	71/0.08	1.0 10^{18}
Latex 4	$PMAA_{38}$-C12	97/3.5	24,350	25,350/1.15	148/0.03	1.2 10^{17}
Latex 5	PAA_{43}-Ac	94/4.3	23,000	24,200/1.69	38/0.16	6.9 10^{18}
Latex 6	PAA_{40}-C4	96/5	23,300	28,300/1.25	51/0.23	3.0 10^{18}
Latex 7	PAA_{46}-C12	95/6	23,100	24,900/1.50	57/0.11	1.9 10^{18}

[a]T = 80°C; SC (Solids Content) ≈ 20%. [KPS] ≈ 2.2 mM. [RAFT]/[I] = 5, except for Latex 6 where the ratio was 5.4. [b]Conversion/time [c]Theoretical M_n calculated from Equation 1. [d]M_n and *Đ* determined by SEC in THF calibrated with polystyrene standards. [e]Z-Average diameter and PdI by DLS. [f]Number of particles per L calculated from $Np = \frac{6 \cdot SC \cdot 10^{22}}{\pi \cdot Z_{av}{}^3 \cdot \rho_{PS}}$ (ρ_{PS} = 1.04 g cm^{-3}).

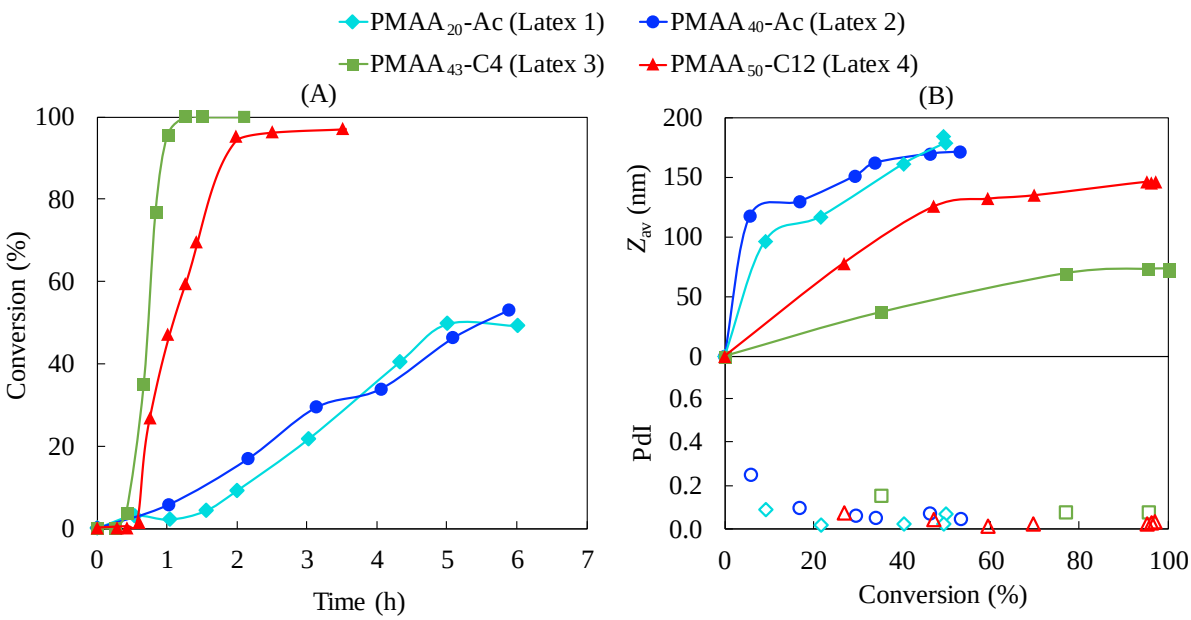

Figure 2 – Conversion-time data for PISA of styrene using PMAA-based macroRAFT with different Z-groups (Latex 1-4, Table 1). (A) Conversion-time data and (B) intensity-mean average diameter (Z_{av}) and dispersity index (PdI).

Before discussing the polymerization mechanism, it is important to address the conformation of PMAA[25, 30] in aqueous solution, and how this can affect the PISA process. Chaduc *et al.*[25] conducted fluorescence studies of short chain PMAA macroRAFT (< 5000 g mol^{-1} with Z-group S-$(CH_2)_2$-CH_3) at different pH. A conformational transition from a PMAA hyper-coiled structure to a water-swollen state was observed between pH 4 and 6. Our group conducted further fluorescence studies to confirm if this change in conformation also applies to PMAA-based macroRAFT with other Z-groups.[30] Interestingly, hyper-coiled PMAA chains were observed under acidic conditions regardless of Z-group hydrophobicity for the Z-groups investigated (-S-$(CH_2)_{11}$-CH_3, -S-$(CH_2)_3$-CH_3, -S-$(CH_2)_3$-COOH). Furthermore, DLS measurements indicated the formation of small aggregates comprising a few chains rather than single chain conformation.

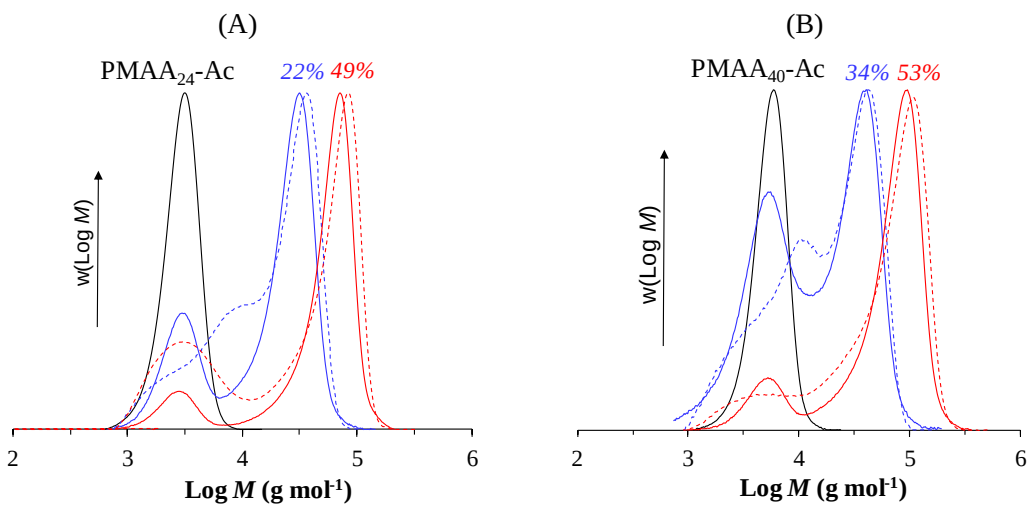

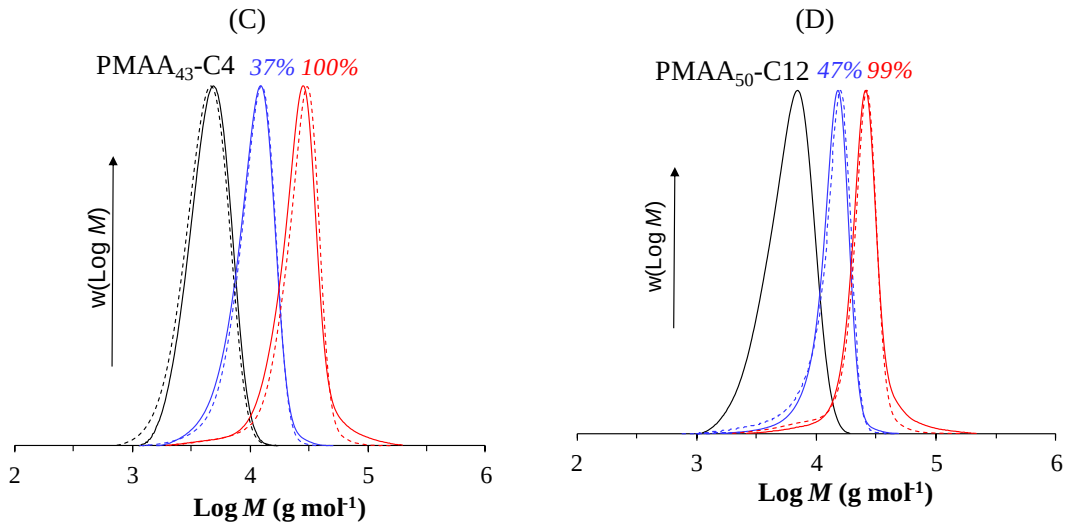

Figure 3 – MWDs of PMAA-*b*-PS block copolymer prepared via PISA using PMAA-based macroRAFT with different Z-groups: (A) $PMAA_{20}$-Ac, (B) $PMAA_{40}$-Ac, (C) $PMAA_{43}$-C4 and (D) $PMAA_{38}$-C12 (Latex 1-4, respectively, Table 1). The number above each MWD indicates the conversion. Straight-lines represent RI signal and dashed-lines the UV-detection (λ = 325 nm).

Returning our attention to the PISA process using $PMAA_{40}$-Ac and $PMAA_{43}$-C4, we propose the mechanism illustrated in Figure 4 to explain the results. It is noteworthy that all polymerizations were performed at acidic conditions (pH < 3) above the critical aggregation concentrations (CAC, a.k.a. CMC; 5.4 x 10^{-6} M ($PMAA_{40}$-Ac) and 2.7 x 10^{-6} M ($PMAA_{43}$-C4)), so hyper-coiled structures are expected to lead to aggregate formation for both macroRAFTs. Step 1 of the mechanism represents this hyper-coiled aggregated structure in aqueous solution. The presence of hydrophobic domains at low pH enhances the local monomer concentration in the vicinity of the PMAA chain end carrying the RAFT moiety leading to rapid chain growth. This behaviour was observed in the system using $PMAA_{43}$-C4, *i.e.* a very fast nucleation step and high polymerization rate (Latex 3 in Figure 2). However, in case of $PMAA_{40}$-Ac, despite the presence of aggregated hydrophobic domains (very similar fluorescence spectrum as $PMAA_{43}$-C4 at pH 3, Figure SI1),[30] slow nucleation and low polymerization rate were observed. We propose that this can be explained by so-called "Z-group induced RAFT exit" due to the more hydrophilic Z-group of $PMAA_{43}$-Ac (Scheme 2). The Z-group RAFT species is the RAFT species generated by addition of a radical having entered the "precursor particle", followed by fragmentation to release a PMAA radical. Exit would occur during the RAFT pre-equilibrium, where the resultant RAFT agent St_n-Z (n = a few units, most likely 1) escapes the hydrophobic domain due to its relatively high hydrophilicity. Such exit results in the loss of RAFT agent from the locus of polymerization, negatively impacting the chain extension. This results in fewer amphiphilic chains being formed, which compromises the colloidal stability, and consequently larger particles form, resulting in a lower total number of particles (Table 1 and Fig. 2B). The reduced rate of chain extension leads to the particles swelling with less St monomer compared to if chain extension were more successful, given chain extension generates hydrophobic PSt domains, which would swell further with St. The polymerization rate is thus negatively impacted both by the lower number of particles (as per established emulsion polymerization kinetics)[33] and by the reduced extent of swelling. Exit of the expelled radical (R-group) has previously been invoked to explain results in both emulsion and miniemulsion polymerization. Importantly, however, such exit refers to the RAFT R-group as a radical species, not the Z-group as part of the RAFT agent

(not a radical) as in the present work – this is a very important distinction. Z-group induced RAFT exit means that the RAFT moiety has exited, unlike R-exit which does not alter the location of the RAFT moiety (*i.e.* the trithiocarbonate moiety in this case). In regards to R-group exit as a radical, Huang *et al.*[34, 35] reported on the emulsion polymerization of St mediated by a PAA-based macroRAFT agent. No polymerization[34] or a long inhibition[35] were observed for this system, which was attributed to exit of the PAA macroradical from the micelle-like structure during the pre-equilibrium step of RAFT process. In fact, the PAA-segment acts as the colloidal stabilizer for the pre-formed particle (or monomer swollen "micelle") and the loss of the macroradical would drastically affect the nucleation step. Macroradical exit has also been observed by other authors[36, 37] in miniemulsion polymerization of St using PAA-based macroRAFT. The macroradical exit mechanism proposed by these authors[34-36] is consistent with our current observations. There are also numerous earlier studies reporting exit of R-group radicals in the case of low MW RAFT agents.[38-42]

The use of a hydrophilic macroRAFT with a lower number of MAA units was also explored, $PMAA_{24}$-Ac (Latex 1 vs Latex 2 of $PMAA_{40}$-Ac). Based on a traditional PISA mechanism one would expect that nucleation would be faster with a shorter hydrophilic block, given that a shorter hydrophobic block would then be sufficient for self-assembly to occur. However, no significant difference was observed when comparing the kinetics of the two systems using St as monomer (Figure 2). This can be rationalized by considering that hydrophobic domains and aggregates (Figure 4) would form also for $PMAA_{24}$-Ac despite its lower molecular weight,[30] and the factor that limits the transformation of "precursor particles" to mature particles is Z-group induced RAFT exit, which restricts the extent of chain extension .

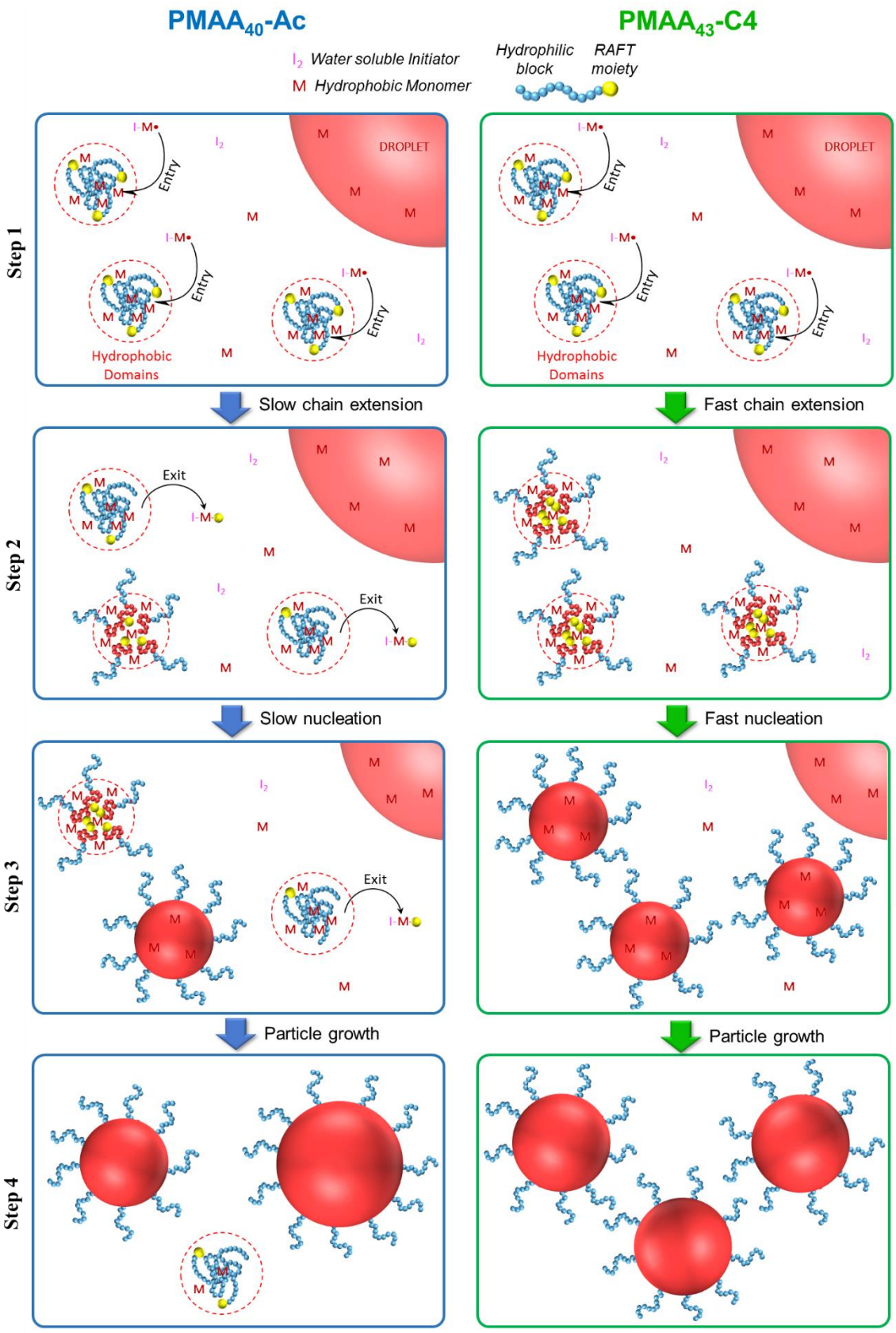

Figure 4 – Schematic illustration of proposed mechanism of particle formation/growth for PISA of St using $PMAA_{40}$-Ac or $PMAA_{43}$-C4 as hydrophilic macroRAFTs (Latex 2 and 3; Table 1). Note that this is merely a schematic illustrating the principles – in reality the mature particles (in red) would comprise a significantly higher number of (blue) chains than displayed. Step 1: Polymerization within monomer-

swollen hydrophobic domains after entry of radical from aqueous phase; Step 2: Chain extension within hydrophobic domains but also significant Z-group induced RAFT exit limiting the extent of chain extension in case of $PMAA_{40}$-Ac; Step 3: The processes of Step 2 continue, accompanied by aggregation of precursor particles and further particle growth, while monomer droplets remain; Step 4: Same as Step 3 but monomer droplets are now depleted.

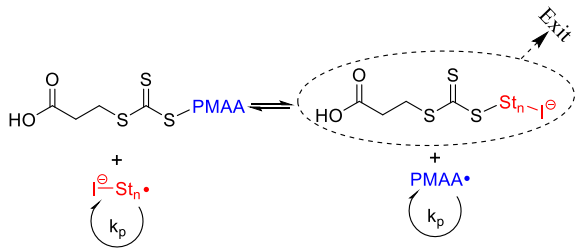

Scheme 2 – Pre-equilibrium of the RAFT mechanism using PMAA-Ac as macroRAFT (Latex 1 and 2, Table 1). "I" represents the sulfate radical anion originating from the initiator potassium persulfate (KPS). The species on the right is referred to as a "Z-group RAFT" species in the text.

It could be speculated that the different mechanisms of particle nucleation for the $PMAA_{43}$-C4 and $PMAA_{40}$-Ac systems may originate in different coil conformations given the different hydrophobicities of the Z-groups. However, in our previous work,[30] we demonstrated that these two macroRAFT species exhibit very similar behaviour in aqueous solution at acidic conditions (all latexes of the current work were prepared at pH < 3). The fluorescence spectra in the presence of Nile red were very similar for the two systems (Figure SI1), indicating that the dye is experiencing similar microenvironments,[30] *i.e.* the same hydrophobic character. Furthermore, the CAC values were also similar as mentioned above. The Z_{av} obtained from DLS for both systems at pH 3 were also very similar, 2.2 and 2.7nm for $PMAA_{43}$-Ac and $PMAA_{41}$-C4, respectively.[30] These results strongly indicate that these two macroRAFT species exhibit similar behaviour in aqueous solution at acidic conditions, although further investigations are necessary to confirm the exact coil conformations.

A PMAA-based macroRAFT containing a more hydrophobic Z-group ($PMAA_{38}$-C12) was also tested (Latex 4, Table 1). Similar to the $PMAA_{43}$-C4 system, the polymerization proceeded fast (Figure 1), reaching 95% in less than 2h. This is in agreement with our proposed mechanism (Figure 4), as the high hydrophobicity of the Z-group (-S-$C_{12}H_{25}$) would prevent Z-group induced RAFT exit. However, a larger particle size was obtained for the $PMAA_{38}$-C12 system (Z_{av} = 148 nm, Latex 4) compared to the $PMAA_{43}$-C4 system (71 nm, Latex 3), although still significantly smaller than for $PMAA_{20}$-Ac (Latex 1; 184 nm) and $PMAA_{40}$-Ac (Latex 2; 190 nm). This difference may be associated with the initial size of the macroRAFT agent in aqueous solution - the $PMAA_{38}$-C12 tends to form a larger aggregate than $PMAA_{43}$-C4, *i.e.* a lower number of precursor particles.[30]

Bimodal MWDs were obtained for the PMAA-based macroRAFT containing the most hydrophilic Z-group, $PMAA_{20}$-Ac and $PMAA_{40}$-Ac (Latex 1 and Latex 2, Figure 3A and Figure 3B, respectively), resulting in very high dispersity ($Đ$ > 2, Table 1). This observation further supports our mechanism, *i.e.* the extent of exit from hydrophobic domains would result in RAFT-end group loss from the polymerization locus (Scheme 2). Hence, the experimental M_n is higher than the $M_{n,th}$ for both systems (Latex 1 and 2, Table 1), indicating unsuccessful RAFT polymerization. In contrast, due to the more hydrophobic character of the Z-groups in $PMAA_{43}$-C4 and $PMAA_{38}$-C12, the absence of such exit results in well-defined shifts toward high molecular weights (Figure 3C and D), $M_n \approx M_{n,th}$ and much lower dispersities (1.29 and 1.15, Table 1) in accordance with a controlled/living polymerization. Furthermore, UV detection (325 nm) resulted in good overlap between the RI and UV signals for Latex 3 and 4 (Figure

3C and D), indicating that the majority of the chains contain the trithiocarbonate RAFT end-group consistent with successful chain extension for $PMAA_{43}$-C4 and $PMAA_{38}$-C12.

PAA-based system: Effect of Z-group hydrophobicity

We decided to further investigate how the hydrophobicity of the Z-group would affect PISA using a more hydrophilic macroRAFT based on acrylic acid. Emulsion polymerizations of styrene were conducted in the presence of PAA_{43}-Ac, PAA_{40}-C4 and PAA_{46}-C12 (Latex 5-7, Table 1). Despite the different Z-groups, similar conversion-time profiles were observed (Figure 5). All polymerizations exhibited long inhibition periods (3-4 h) followed by very rapid polymerization after nucleation, reaching full conversion in less than 1 h after nucleation. One may anticipate that the longer inhibition period for PAA would be caused by its higher hydrophilicity compared to the PMAA systems, considering that a longer polystyrene block would be required before self-assembly. However, it was demonstrated above for the PMAA system that the length of the hydrophilic block does not have any significant impact on the kinetics, suggesting that the difference between PAA and PMAA systems would most likely be associated with presence of hydrophobic domains (hyper-coiled state of PMAA) at the early stages of the polymerization.[25]

Chaduc *et al.*[24] showed that PAA macroRAFT chains do not exhibit a hyper-coiled structure at low pH by use of fluorescence studies. Our recent work[30] confirms this behaviour, showing that regardless of the Z-group, significant hydrophobic domains were not observed at pH 3 for PAA-based macroRAFT species. Therefore, there are no aggregates present before polymerization and nucleation depends solely on chain extension and subsequent self-assembly. Since there are no significant hydrophobic domains, the local monomer concentration in the vicinity of the non-coiled PAA active chain is reduced dramatically due to the lower styrene concentration in water (schematically illustrated in Figure 6).[24] This leads to a much slower growth of the PSt block and therefore a long inhibition period to reach the critical chain length required for self-assembly. An additional factor that may also affect the nucleation step is the fragmentation of the intermediate radical in favour of the polystyryl radical ("backwards fragmentation") rather than the PAA radical during the RAFT pre-equilibrium, which would also delay the nucleation step. However, once the growing macroRAFT reached the critical PSt length, a very high number of particles is generated (~10^{18} L^{-1}, Table 1), which correlates directly with the small particle size for all PAA-based systems (<60 nm, Figure 5), leading to very rapid polymerization.

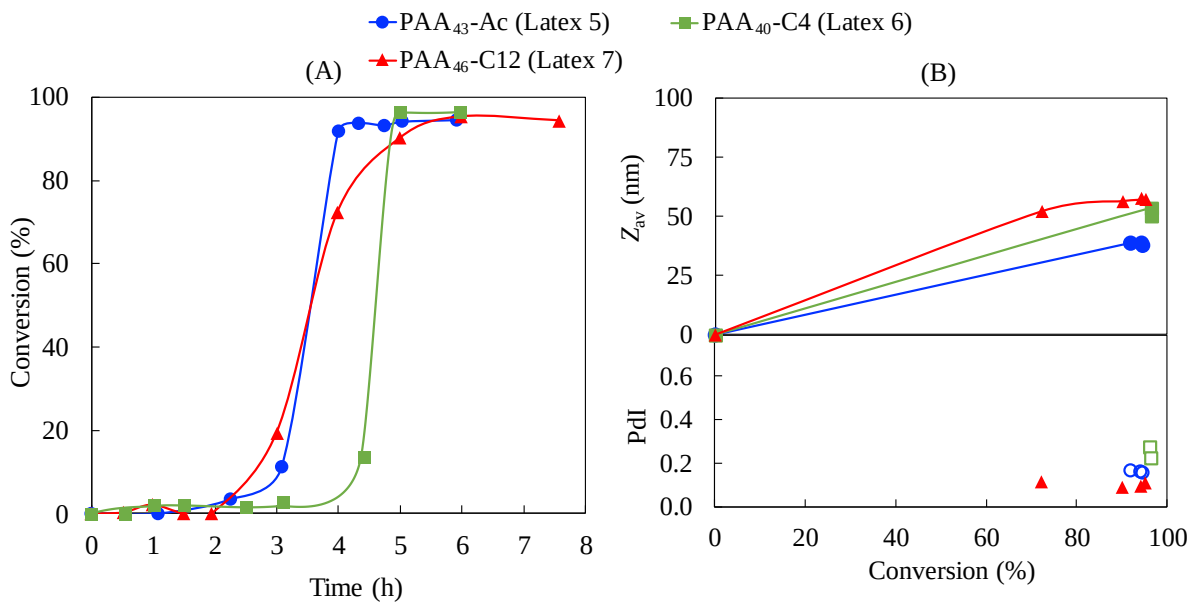

Figure 5 – Conversion-time data (A) and intensity-mean average diameter (Z_{av}, lines added as guide to the eye) and dispersity index (PdI) (B) for PISA of styrene using PMAA- and PAA-based macroRAFT with different Z-groups (Latex 1-5, Table 1).

The long inhibition period for PAA systems (Latex 5-7) also results in less effective chain extension compared to the PMAA-based systems. SEC-traces for both PAA systems (Figure 7) exhibit low MW tailing, which can be associated with dead chains generated during the long inhibition period. The more pronounced effect in the PAA_{43}-Ac system (Latex 5) may be associated with the extent of Z-group induced RAFT exit due to the higher hydrophilicity of the Z-group. In the PAA-system, the particle from which exit occurs comprises PAA-*b*-PSt, hence the PAA-*b*-PSt macroRAFT is unable to exit, but the RAFT agent generated via addition-fragmentation involving the entering radical is much more hydrophilic. As mentioned above for the PAA_{46}-C12 system, macroradical exit ($PAA^{\bullet}$) may also be taking place, which would negatively impact the formation of block copolymer.[34-36] A common way to minimize the number of dead chains in RAFT is to reduce the initiator concentration.[43-45] We performed two polymerizations using PAA_{40}-C4 with lower initiator concentration ([RAFT]/[I] = 10 and 20, Figure SI2). However, less than 10% conversion was observed in 23h, which originates in the low polymerization rate in the aqueous phase, thereby delaying nucleation.

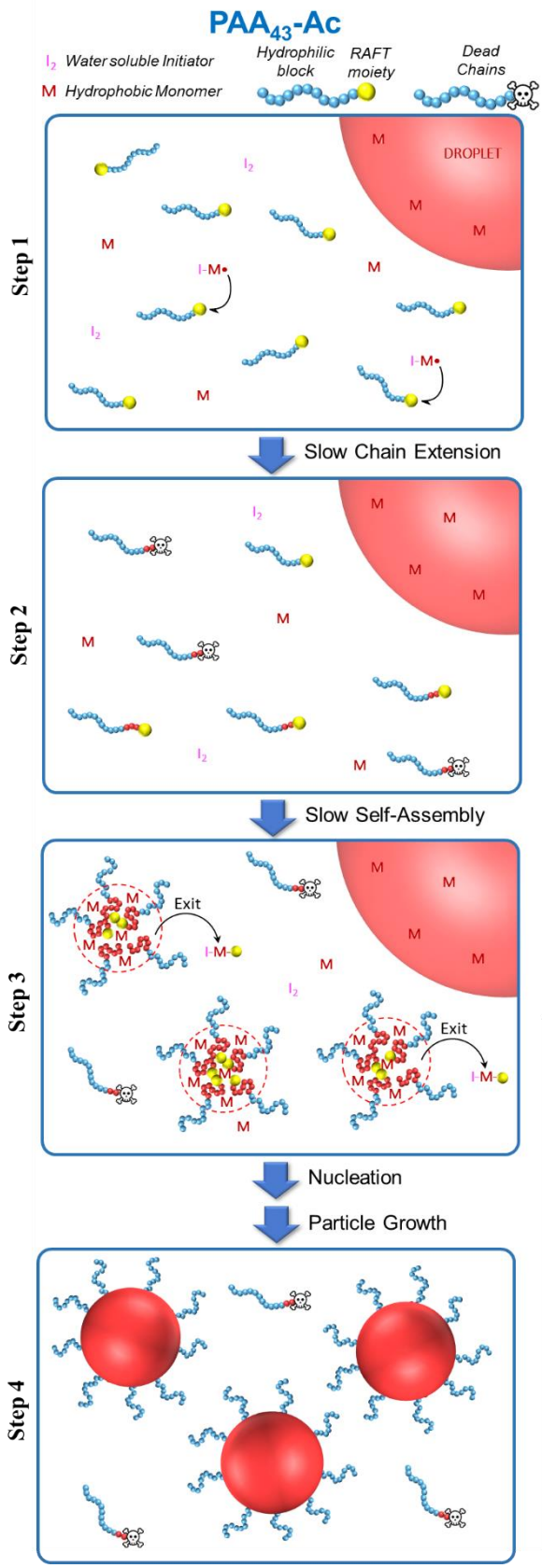

Figure 6 – Schematic illustration of proposed mechanism of particle nucleation and growth for PISA polymerization of styrene using PAA_{43}-Ac as hydrophilic macroRAFT (Latex 5, Table 1). Steps 1 and 2: Polymerization in the aqueous phase, generating some dead chains; Step 3: Nucleation accompanied by some Z-group induced RAFT exit; Step 4: Particle growth with monomer droplets being depleted.

(A)

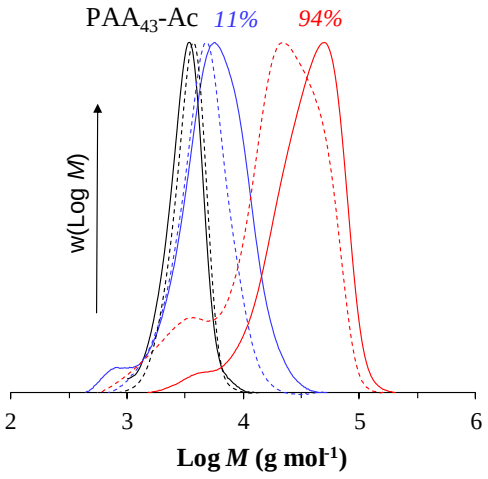
PAA43-Ac 11% 94%
w(Log M)
2
3
4
5
6
Log M (g mol-1)

(B)

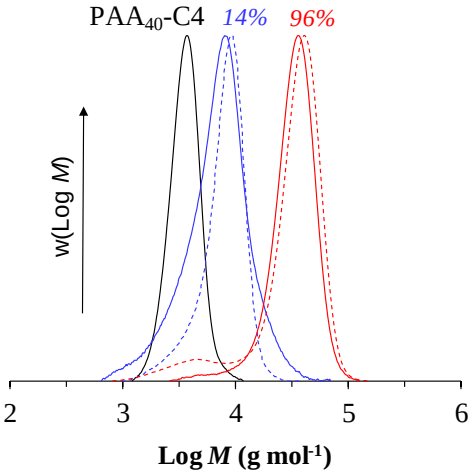
PAA40-C4 14% 96%
w(Log M)
2
3
4
5
6
Log M (g mol-1)

(C)

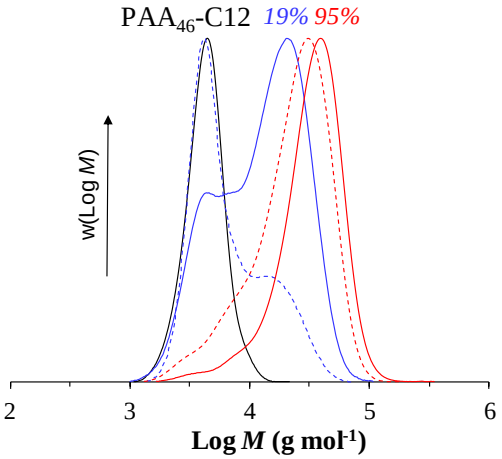
PAA46-C12 19% 95%
w(Log M)
2
3
4
5
6
Log M (g mol-1)

Figure 7 – THF-SEC traces of PAA-*b*-PS block copolymer prepared via PISA using PAA-based macroRAFT with different Z-groups: (A) PAA_{43}-Ac and (B) $PMAA_{40}$-C4 (Latex 5-7, respectively, Table 1). The number above each MWD indicates the monomer conversion.

CONCLUSIONS

The nucleation (particle formation) process in RAFT PISA implemented as an emulsion polymerization has been examined with respect to the effect of the Z-group of hydrophilic macroRAFT agents based on acrylic acid (AA) and methacrylic acid (MAA). Surprisingly, the polymerization of styrene mediated by PMAA-Ac (macroRAFT using the more hydrophilic Z-group) led to low polymerization rates, poor chain extension and relatively large particles. On the other hand, when polymerizations were performed in the presence of PMAA-based macroRAFTs with more hydrophobic Z-groups, $PMAA_{43}$-C4 and $PMAA_{38}$-C12, high rates were observed resulting in full conversion, efficient chain extension and small particles.

A mechanism based on so-called Z-group induced RAFT exit is proposed to explain these different behaviours. Z-group induced RAFT exit refers to the RAFT agent generated by addition of a radical to the initial macroRAFT followed by "forward" fragmentation, resulting in a new RAFT agent where the initial PAA or PMAA segment has been replaced by an entering radical. The more hydrophilic character of the Z-group for PMAA-Ac (in combination with the R-group being a small moiety of relatively high hydrophilicity) leads to high probability of exit from the hydrophobic domains during the nucleation step, causing loss of the RAFT moiety. This ultimately leads to low polymerization rate, poor chain extension and, consequently, low degree of livingness.[46] Z-group induced RAFT exit is also proposed to occur in PAA-based systems, leading to poor chain extension for PAA_{43}-Ac while successful chain extension was observed for PAA_{40}-C4 and PAA_{46}-C12 (the latter two with more hydrophobic Z-groups). At low pH (all polymerizations in this study), PMAA chains form hyper-coiled structures as aggregates comprising a few chains which swell with hydrophobic monomer (the second block). Such behaviour is not exhibited by PAA. Consequently, the nucleation process (and thereby the time taken to reach high monomer conversion) is much slower for PAA-based systems because the local monomer concentration is not enhanced as it is for PMAA-based systems.

Overall, these results demonstrate that (*i*) PMAA-based macroRAFTs are preferable over PAA-based macroRAFTs, and (*ii*) the Z-group of the macroRAFT should be sufficiently hydrophobic for successful implementation of RAFT PISA as an aqueous emulsion polymerization. These findings have important implications for further development and optimization of PISA processes for synthesis of polymeric nanoparticles. Moreover, these systems are of a great interest for the preparation of multiblock copolymers[47, 48] – investigations are currently underway and will be reported in forthcoming publications.

REFERENCES

1. Charleux, B.; Delaittre, G.; Rieger, J.; D'Agosto, F., Polymerization-induced self-assembly: from soluble macromolecules to block copolymer nano-objects in one step. *Macromolecules* **2012,** *45* (17), 6753-6765.
2. Rieger, J., Guidelines for the synthesis of block copolymer particles of various morphologies by RAFT dispersion polymerization. *Macromolecular rapid communications* **2015,** *36* (16), 1458-1471.
3. Derry, M. J.; Fielding, L. A.; Armes, S. P., Polymerization-induced self-assembly of block copolymer nanoparticles via RAFT non-aqueous dispersion polymerization. *Progress in Polymer Science* **2016,** *52*, 1-18.
4. Canning, S. L.; Smith, G. N.; Armes, S. P., A critical appraisal of RAFT-mediated polymerization-induced self-assembly. *Macromolecules* **2016,** *49* (6), 1985-2001.
5. Lansalot, M.; Rieger, J., Polymerization ‐ Induced Self ‐ Assembly. *Macromolecular rapid communications* **2019,** *40* (2), 1800885.
6. Penfold, N. J. W.; Yeow, J.; Boyer, C.; Armes, S. P., Emerging Trends in Polymerization-Induced Self-Assembly. *ACS Macro Letters* **2019,** *8* (8), 1029-1054.
7. Liu, C.; Hong, C.-Y.; Pan, C.-Y., Polymerization techniques in polymerization-induced self-assembly (PISA). *Polymer Chemistry* **2020,** *11* (22), 3673-3689.
8. Zhou, D.; Kuchel, R. P.; Zetterlund, P. B., A new paradigm in polymerization induced self-assembly (PISA): Exploitation of "non-living" addition–fragmentation chain transfer (AFCT) polymerization. *Polymer Chemistry* **2017,** *8* (29), 4177-4181.
9. Chong, Y.; Le, T. P.; Moad, G.; Rizzardo, E.; Thang, S. H., A more versatile route to block copolymers and other polymers of complex architecture by living radical polymerization: the RAFT process. *Macromolecules* **1999,** *32* (6), 2071-2074.
10. McCormick, C. L.; Lowe, A. B., Aqueous RAFT polymerization: recent developments in synthesis of functional water-soluble (co) polymers with controlled structures. *Accounts of chemical research* **2004,** *37* (5), 312-325.
11. Zetterlund, P. B.; Kagawa, Y.; Okubo, M., Controlled/living radical polymerization in dispersed systems. *Chemical reviews* **2008,** *108* (9), 3747-3794.
12. Khor, S. Y.; Quinn, J. F.; Whittaker, M. R.; Truong, N. P.; Davis, T. P., Controlling Nanomaterial Size and Shape for Biomedical Applications via Polymerization ‐ Induced Self ‐ Assembly. *Macromolecular rapid communications* **2019,** *40* (2), 1800438.
13. Zhang, W. J.; Hong, C. Y.; Pan, C. Y., Polymerization ‐ Induced Self ‐ Assembly of Functionalized Block Copolymer Nanoparticles and Their Application in Drug Delivery. *Macromolecular rapid communications* **2019,** *40* (2), 1800279.
14. Lesage de la Haye, J.; Martin-Fabiani, I.; Schulz, M.; Keddie, J. L.; D'agosto, F.; Lansalot, M., Hydrophilic MacroRAFT-mediated emulsion polymerization: Synthesis of latexes for cross-linked and surfactant-free films. *Macromolecules* **2017,** *50* (23), 9315-9328.
15. Martín-Fabiani, I.; Lesage de la Haye, J.; Schulz, M.; Liu, Y.; Lee, M.; Duffy, B.; D'Agosto, F.; Lansalot, M.; Keddie, J. L., Enhanced Water Barrier Properties of Surfactant-Free Polymer Films Obtained by MacroRAFT-Mediated Emulsion Polymerization. *ACS applied materials & interfaces* **2018,** *10* (13), 11221-11232.
16. Upadhyaya, L.; Egbosimba, C.; Qian, X.; Wickramasinghe, R.; Fernández ‐ Pacheco, R.; Coelhoso, I. M.; Portugal, C. A.; Crespo, J. G.; Quemener, D.; Semsarilar, M., Influence of Magnetic Nanoparticles on PISA Preparation of Poly (Methacrylic Acid) ‐ b ‐ Poly (Methylmethacrylate) Nano ‐ Objects. *Macromolecular rapid communications* **2019,** *40* (2), 1800333.
17. Boussiron, C.; Le Bechec, M.; Petrizza, L.; Sabalot, J.; Lacombe, S.; Save, M., Synthesis of Film-Forming Photoactive Latex Particles by Emulsion Polymerization–Induced Self-Assembly to Produce Singlet Oxygen. *Macromolecular Rapid Communications* **2019,** *40* (2), 1800329.

18. Richardson, R. A. E.; Guimarães, T. R.; Khan, M.; Moad, G.; Zetterlund, P. B.; Perrier, S., Low-Dispersity Polymers in *Ab Initio* Emulsion Polymerization: Improved MacroRAFT Agent Performance in Heterogeneous Media. *Macromolecules* **2020**. (DOI: 10.1021/acs.macromol.0c01311)
19. Zhou, D.; Dong, S.; Kuchel, R. P.; Perrier, S.; Zetterlund, P. B., Polymerization induced self-assembly: tuning of morphology using ionic strength and pH. *Polymer Chemistry* **2017,** *8* (20), 3082-3089.
20. Zhou, D.; Kuchel, R. P.; Dong, S.; Lucien, F. P.; Perrier, S.; Zetterlund, P. B., Polymerization‐Induced Self‐Assembly under Compressed CO2: Control of Morphology Using a CO2‐Responsive MacroRAFT Agent. *Macromolecular rapid communications* **2019,** *40* (2), 1800335.
21. Ferguson, C. J.; Hughes, R. J.; Nguyen, D.; Pham, B. T.; Gilbert, R. G.; Serelis, A. K.; Such, C. H.; Hawkett, B. S., Ab initio emulsion polymerization by RAFT-controlled self-assembly. *Macromolecules* **2005,** *38* (6), 2191-2204.
22. Ferguson, C. J.; Hughes, R. J.; Pham, B. T.; Hawkett, B. S.; Gilbert, R. G.; Serelis, A. K.; Such, C. H., Effective ab initio emulsion polymerization under RAFT control. *Macromolecules* **2002,** *35* (25), 9243-9245.
23. Chaduc, I.; Zhang, W.; Rieger, J.; Lansalot, M.; D'Agosto, F.; Charleux, B., Amphiphilic Block Copolymers from a Direct and One‐pot RAFT Synthesis in Water. *Macromolecular rapid communications* **2011,** *32* (16), 1270-1276.
24. Chaduc, I.; Crepet, A. s.; Boyron, O.; Charleux, B.; D'Agosto, F.; Lansalot, M., Effect of the pH on the RAFT polymerization of acrylic acid in water. Application to the synthesis of poly (acrylic acid)-stabilized polystyrene particles by RAFT emulsion polymerization. *Macromolecules* **2013,** *46* (15), 6013-6023.
25. Chaduc, I.; Girod, M.; Antoine, R.; Charleux, B.; D'Agosto, F.; Lansalot, M., Batch emulsion polymerization mediated by poly (methacrylic acid) macroRAFT agents: one-pot synthesis of self-stabilized particles. *Macromolecules* **2012,** *45* (15), 5881-5893.
26. Carlsson, L.; Fall, A.; Chaduc, I.; Wågberg, L.; Charleux, B.; Malmström, E.; D'Agosto, F.; Lansalot, M.; Carlmark, A., Modification of cellulose model surfaces by cationic polymer latexes prepared by RAFT-mediated surfactant-free emulsion polymerization. *Polymer Chemistry* **2014,** *5* (20), 6076-6086.
27. Chaduc, I.; Reynaud, E.; Dumas, L.; Albertin, L.; d'Agosto, F.; Lansalot, M., From well-defined poly (N-acryloylmorpholine)-stabilized nanospheres to uniform mannuronan-and guluronan-decorated nanoparticles by RAFT polymerization-induced self-assembly. *Polymer* **2016,** *106*, 218-228.
28. Cockram, A. A.; Neal, T. J.; Derry, M. J.; Mykhaylyk, O. O.; Williams, N. S.; Murray, M. W.; Emmett, S. N.; Armes, S. P., Effect of monomer solubility on the evolution of copolymer morphology during polymerization-induced self-assembly in aqueous solution. *Macromolecules* **2017,** *50* (3), 796-802.
29. Brotherton, E. E.; Hatton, F. L.; Cockram, A. A.; Derry, M. J.; Czajka, A.; Cornel, E. J.; Topham, P. D.; Mykhaylyk, O. O.; Armes, S. P., In situ small-angle X-ray scattering studies during reversible addition–fragmentation chain transfer aqueous emulsion polymerization. *Journal of the American Chemical Society* **2019,** *141* (34), 13664-13675.
30. Thompson, S. W.; Guimaraes, T. R.; Zetterlund, P. B., RAFT Emulsion Polymerization: MacroRAFT Agent Self-Assembly Investigated Using a Solvachromatic Dye. *Biomacromolecules* **2020**.
31. Le-Masurier, S. P.; Duong, H. T. T.; Boyer, C.; Granville, A. M., Surface modification of polydopamine coated particles via glycopolymer brush synthesis for protein binding and FLIM testing. *Polymer Chemistry* **2015,** *6* (13), 2504-2511.
32. Moad, G., A Critical Assessment of the Kinetics and Mechanism of Initiation of Radical Polymerization with Commercially Available Dialkyldiazene Initiators. *Progress in Polymer Science* **2018**.
33. Thickett, S. C.; Gilbert, R. G., Emulsion polymerization: State of the art in kinetics and mechanisms. *Polymer* **2007,** *48* (24), 6965-6991.

34. Huang, J.; Zhao, S.; Gao, X.; Luo, Y.; Li, B., RAFT Ab Initio Emulsion Polymerization of Styrene Using Poly (acrylic acid) ‐ b ‐ polystyrene Trithiocarbonate of Various Structures as Mediator and Surfactant. *Macromolecular Reaction Engineering* **2014,** *8* (10), 696-705.
35. Huang, J.; Zhao, S.; Gao, X.; Luo, Y.; Li, B., Ab initio RAFT emulsion copolymerization of styrene and acrylonitrile. *Industrial & Engineering Chemistry Research* **2014,** *53* (18), 7688-7695.
36. Butté, A.; Storti, G.; Morbidelli, M., Miniemulsion Living Free Radical Polymerization by RAFT. *Macromolecules* **2001,** *34* (17), 5885-5896.
37. Monteiro, M. J.; Hodgson, M.; De Brouwer, H., The influence of RAFT on the rates and molecular weight distributions of styrene in seeded emulsion polymerizations. *Journal of Polymer Science Part A: Polymer Chemistry* **2000,** *38* (21), 3864-3874.
38. Lansalot, M.; Davis, T. P.; Heuts, J. P., RAFT miniemulsion polymerization: Influence of the structure of the RAFT agent. *Macromolecules* **2002,** *35* (20), 7582-7591.
39. Luo, Y.; Liu, B.; Wang, Z.; Gao, J.; Li, B., Butyl acrylate RAFT polymerization in miniemulsion. *Journal of Polymer Science Part A: Polymer Chemistry* **2007,** *45* (11), 2304-2315.
40. Peklak, A. D.; Butté, A., Kinetic model of reversible addition fragmentation chain transfer polymerization of styrene in seeded emulsion. *Journal of Polymer Science Part A: Polymer Chemistry* **2006,** *44* (20), 6114-6135.
41. Prescott, S. W.; Ballard, M. J.; Rizzardo, E.; Gilbert, R. G., Rate optimization in controlled radical emulsion polymerization using RAFT. *Macromolecular theory and simulations* **2006,** *15* (1), 70-86.
42. Yingwu, L., Monte Carlo Simulations for the Very Beginning of RAFT Seeded Emulsion Polymerization. *Chemical Journal of Chinese Universities* **2003,** *24* (10), 1926-1928.
43. Gody, G.; Maschmeyer, T.; Zetterlund, P. B.; Perrier, S., Rapid and quantitative one-pot synthesis of sequence-controlled polymers by radical polymerization. *Nature communications* **2013,** *4*, ncomms3505.
44. Gody, G.; Maschmeyer, T.; Zetterlund, P. B.; Perrier, S., Exploitation of the degenerative transfer mechanism in RAFT polymerization for synthesis of polymer of high livingness at full monomer conversion. *Macromolecules* **2014,** *47* (2), 639-649.
45. Gody, G.; Maschmeyer, T.; Zetterlund, P. B.; Perrier, S. b., Pushing the limit of the RAFT process: multiblock copolymers by one-pot rapid multiple chain extensions at full monomer conversion. *Macromolecules* **2014,** *47* (10), 3451-3460.
46. Khan, M.; Guimarães, T. R.; Zhou, D.; Moad, G.; Perrier, S.; Zetterlund, P. B., Exploitation of Compartmentalization in RAFT Miniemulsion Polymerization to Increase the Degree of Livingness. *Journal of Polymer Science Part A: Polymer Chemistry* **2019,** *57* (18), 1938-1946.
47. Clothier, G. K.; Guimarães, T. R.; Khan, M.; Moad, G.; Perrier, S. b.; Zetterlund, P. B., Exploitation of the nanoreactor concept for efficient synthesis of multiblock copolymers via macroRAFT-mediated emulsion polymerization. *ACS Macro Letters* **2019,** *8* (8), 989-995.
48. Guimarães, T. R.; Khan, M.; Kuchel, R. P.; Morrow, I. C.; Minami, H.; Moad, G.; Perrier, S. b.; Zetterlund, P. B., Nano-Engineered Multiblock Copolymer Nanoparticles via Reversible Addition–Fragmentation Chain Transfer Emulsion Polymerization. *Macromolecules* **2019,** *52* (8), 2965-2974.